Characterization of a Previously Unidentified Viral Protein in Porcine Circovirus Type 2-Infected Cells and Its Role in Virus-Induced Apoptosis

Jue Liu, Isabelle Chen, and Jimmy Kwang*

Animal Health Biotechnology Group, Temasek Life Sciences Laboratory, National University of Singapore, 1 Research Link, Singapore 117604

Porcine circovirus type 2 (PCV2) is the causative agent of postweaning multisystemic wasting syndrome in pigs. In this study, transcription and translation of a novel viral gene (termed ORF3 here) was detected during productive infection of PCV2 in PK15 cells. The results of infection with ORF3-deficient PCV2 by site-directed mutagenesis indicated that the protein is not essential for viral replication. To investigate the underlying mechanism of cell death caused by replication of PCV2, apoptosis characterized by chromosomal condensation and fragmentation, formation of apoptotic bodies, and significant increase in hypodiploids were detected in infected cells. We further demonstrated that PCV2-induced apoptosis required the activation of caspase-8 but not caspase-9. The activation of caspase-8 results in the activation of caspase-3 as shown by an increase in the cleavage of the caspase substrate in the infected cells. To determine whether ORF3 protein could trigger apoptosis, ORF3 as well as ORF1 and ORF2 genes were transiently expressed in PK15 and Cos-7 cells for apoptotic activity assay. Transfection of cells with the ORF3 alone induced apoptosis using a pathway similar to that described in the context of viral infection. This is further confirmed by a significant decrease in apoptotic activity of infected cells in the absence of the ORF3 expression, suggesting that the protein plays a major role in the induction of virus-induced apoptosis. Altogether, these results indicate that ORF3 is a novel PCV2 protein that is not essential for viral replication in cultured cells but is involved in PCV2-induced apoptosis by activating caspase-8 and caspase-3 pathways.

Porcine circovirus (PCV) was originally identified as a contaminant of porcine kidney cell cultures (PK15, ATCC CCL-33) (47). The PCV virion is icosahedral, nonenveloped, and 17 nm in diameter. The genome of PCV is a single-stranded circular DNA of about 1.76 kb. PCV is classified in the genus *Circovirus* of the *Circoviridae* family, which consists of other animal circoviruses such as psittacine beak-feather disease virus, goose circovirus, canary circovirus, and pigeon circovirus (35, 38, 50–52). Chicken anemia virus has been assigned to the new genus *Gyrovirus* of this family (36), and it shares similar characteristics with the human TT virus (28, 33) and TTV-like minivirus (44). Two genotypes of PCV have been recognized. The PK15 cell-derived PCV has been considered to be nonpathogenic to pigs (3, 48) and is designated PCV type 1 (PCV1). Serologic surveys indicated that PCV1 is widespread in swine, but no known animal disease has been associated with PCV1. On the other hand, PCV type 2 (PCV2) is now accepted as the major infectious agent involved in postweaning multisystemic wasting syndrome (PMWS) (2, 6, 20), a new emerging swine disease worldwide since its occurrence in Canada in 1991 (1, 8).

PMWS primarily affects pigs between 5 and 18 weeks of age. Clinical PMWS signs include progressive weight loss, dyspnea, tachypnea, anemia, diarrhea, and jaundice. Mortality rates may vary from 1 to 2% up to 30% in complicated cases. Microscopic lesions are characterized by lymphocyte depletion of follicular and interfollicular areas together with macrophage infiltration of lymphoid tissues in PMWS-affected pigs. PMWS is now endemic in many swine-producing countries, causing a potential economical impact on the swine industry worldwide.

Apoptosis is an active physiological process of cellular self-destruction with specific morphological and biochemical changes (39). External apoptotic stimuli and signals generated from within the cell can activate signal transduction pathways involving a family of cysteine proteases (caspases) that play a central role in apoptosis (11, 40). Caspases have been divided into initiators and effectors based on their place in the caspase cascade. The initiators (caspase-8, caspase-9, and caspase-10) are activated by their own intrinsic autocatalytic activity with the help of other proteins with which they form complexes known as apoptosomes (16). The effectors (caspase-3, caspase-6, and caspase-7) are activated via the action of the initiators and are responsible for the characteristic morphological changes of apoptosis. Initiating events of the caspase cascade have been well characterized, one of which is the FADD (Fas-associating protein with death domain) adaptor-mediated recruitment of procaspase-8 to Fas-ligand-bound, multimerized Fas receptors (CD95 and Apo-1), leading to caspase-8 activation consecutively resulting in cleavage of the effector caspase-3 and caspase-7 (4, 41).

Many viruses induce apoptosis as part of their natural life cycle (39). On the one hand, apoptosis may be an important mechanism for the release and dissemination of host-cell-produced progeny virions by minimizing inflammatory or immune responses to the viral agent. On the other hand, virus-induced

* Corresponding author. Mailing address: Animal Health Biotechnology Group, Temasek Life Sciences Laboratory, National University of Singapore, 1 Research Link, Singapore 117604. Phone: (65) 68727473. Fax: (65) 68727007. E-mail: kwang@tll.org.sg.

apoptosis could be regarded as a defense strategy of multicellular host organisms for the purposeful destruction of infected cells. Most viruses that lead to apoptotic cell death trigger the activation of the caspase cascade for the execution process of the death program. Apoptosis has been proposed as the mechanism that is responsible for B-cell depletion in naturally PMWS-affected pigs (43), but contradictory studies have recently reported that lymphocyte apoptosis is not a prevalent phenomenon in the development of PMWS lymphoid depletion lesions (24, 37).

The overall DNA sequence homology within the PCV1 or PCV2 isolates is greater than 90%, while the homology between PCV1 and PCV2 isolates is 68 to 76%. Two major open reading frames (ORFs) have been recognized for PCV, ORF1, called the *rep* gene, which encodes a protein of 35.7 kDa involved in virus replication (26), and ORF2, called the *cap* gene, which encodes the major immunogenic capsid protein of 27.8 kDa (9, 30, 31). In addition to the replicase ORF1 and the capsid protein ORF2, it is predicted to contain another five potential ORFs encoding proteins larger than 5 kDa by computer searching (27). Whether these potential ORFs are expressed or not and whether the expressed proteins are essential for viral replication await elucidation. For PCV2, the largest among these is the fragment of 315 bp in length, called ORF3 here, which does not show similarities to any known protein. In contrast, the ORF fragment located in corresponding region of PCV1 is 612 bp in length, much longer than ORF3 in PCV2. Furthermore, there is only 61.5% amino acid identity between the ORF3 of PCV2 and the corresponding region of PCV1. Whether the variation is associated with PCV2 pathogenicity has not been determined.

In the present study, we used a specific antibody against ORF3 to show that it is indeed expressed in PCV2-infected cells and that it is not essential for PCV2 replication in cultured cells. We then characterized that PCV2 could induce apoptosis in cultured PK15 cells by activating initiator caspase-8 and effector caspase-3 pathways. Moreover, the ORF3 protein has been shown to play a major role in PCV2-induced apoptosis using a pathway similar to that described in the context of viral infection. This is further confirmed by a significant decrease in apoptotic activity of infected cells in the absence of ORF3 expression.

MATERIALS AND METHODS

Virus and cells. The permanent PK15 cell line, which was free of PCV, was maintained in minimal essential medium (Gibco) supplemented with 5% heat-inactivated fetal bovine serum, 5% L-glutamine, 100 U/ml of penicillin G, and 100 μl/ml streptomycin at 37°C in a humidified 5% CO_2 incubator. Cos-7 cells, used for transient expression assay, were maintained in Dulbecco's modified Eagle's medium (Gibco) supplemented with 10% fetal bovine serum. The PCV2 virus strain BJW used in the study was originally isolated from a kidney tissue sample of a pig with naturally occurring PMWS in the North region of China. The kidney tissues were treated and inoculated into PK15 cells.

Raising antibody to ORF3. As shown in Fig. 1A, ORF1 and ORF2 as well as ORF3 genes are indicated in the genetic map of the PCV2 strain BJW. The DNA encoding full-length ORF3 was cloned into PQE30 and transformed into *Escherichia coli* BL21 cells. These cells were induced to express ORF3 with IPTG (isopropyl-β-D-thiogalactopyranoside) and allowed to grow for 4 h at 37°C. His-tagged fusion protein was purified, and the preparation was injected into mice for raising polyclonal antibody. After four injections, the mice were bled, and the sera were tested for reactivity to ORF3. The antibody showed specific reactivity to ORF3 expressed in PK15 cells infected with the PCV2 virus or transfected with an ORF3 expression construct.

Construction of PCV2 mutant and plasmids. A pair of PCR primers were designed according to the sequence of the PCV2 isolate strain BJW: forward primer F-PCVPST (5′-TGCACTGCAGTAAAGAAGGCAACTTAC-3′) and reverse primer R-PCVPST (5′-TGCACTGCAGTATTCTTTATTCTGCTG-3′). This pair of primers amplifies the complete genome of PCV2 with an overlapping region containing the unique PstI restriction enzyme site (Fig. 1A). Briefly, DNA was extracted using the QIAamp DNA Minikit (QIAGEN) from a kidney tissue sample of a pig with naturally occurring PMWS. The extracted DNA was amplified by PCR machine (Perkin-Elmer). The PCR consisted of an initial enzyme activation step at 94°C for 5 min followed by 35 cycles of denaturation at 94°C for 1 min, annealing at 48°C for 1 min, extension at 72°C for 2 min, and a final extension at 72°C for 10 min. The PCR product of expected size was separated by gel electrophoresis and purified using a PCR purification kit (QIAGEN).

To construct a molecular DNA clone containing the PCV2 genome, the PCR product was cloned into the pBlueScript SK (pSK) vector. The clone was sequenced on both strands by using the M13 forward and reverse universal primers as well as PCV2 genome-specific primers and the ABI Prism Dye Terminator cycle sequencing kit (PE Biosystems).

Specific mutation was introduced into the cloned PCV2 genome using the QuickChange site-directed mutagenesis kit (Strategene). Mutant plasmid was generated with a set of mutagenesis primers (forward primer, 5′-GGGATGGT TACCAC*G*GTGAAGTGGTTGTTA-3′; reverse primer, TAACAACCACTTC TTCACC*G*TGGTAACCATCCC-3′) according to the manufacturer's instructions. The mutation (nucleotide [nt] 671) is indicated in italic letters and cannot change amino acids of ORF1 protein at the site. After the PCV2 genome was excised from the pSK plasmid and circularized by ligation, the ligated DNA mixture was transfected into approximately 60 to 80% confluent PK15 cells.

To prepare recombinant eukaryotic expression plasmids, the coding sequences of ORF1, ORF2, and ORF3 genes were amplified from the PCV2 genome. The primers GFP-ORF1(5) (5′-CCGCTCGAGCTATGCCCAGCAAGAAGAATG G-3′) and GFP-ORF1(3) (5′-CGGGGTACCTCAGTAATTTATTTCATATG-3′), GFP-ORF2(5) (5′-CCCAAGCTTCGATGACGTACCCAAGGAGGCG-3′) and GFP-ORF2(3) (5′-CGGGGTACCTTATGGTTTAAGTGGGGGGTC-3′), and GFP-ORF3(5) (5′-CCCAAGCTTCGATGGTAACCATCCCACCACT TG-3′) and GFP-ORF3(3) (5′-CGGGGTACCTTACTTATCGAGTGTGGAG CTC-3′) were used to amplify these three genes, respectively. The XhoI/KpnI fragment of ORF1 and HindIII/KpnI fragments of ORF2 and ORF3 were directionally cloned into the corresponding sites of eukaryotic expression vector pEGFP-C1 (Clontech), downstream of the human cytomegalovirus promoter, to obtain green fluorescent protein (GFP)-ORF1, GFP-ORF2 and GFP-ORF3, respectively. They were sequenced to confirm that no errors were introduced as a result of PCR amplification.

Transfection and infection. For genome transfections, PstI-digested PCV2 or ORF3-deficient PCV2 for generating recombinant PCV2 (rPCV2) or mutant PCV2 (rPCV3Δ), respectively, obtained from the corresponding cloned genomes, was gel purified and recircularized in the presence of T4 DNA ligase (BioLab) overnight at 16°C before being transfected. Cells were additionally treated with 300 mM D-glucosamine at 24 h after transfection as described previously (49). For the infection test, the genome-transfected cells were subjected to three successive freeze-thaw cycles. The total lysates were collected and used to infect PCV-free PK15 cells. They were then subjected to glucosamine treatment as described above and analyzed by indirect fluorescence assay (IFA) after infection.

In vitro expression of the GFP-ORF1, GFP-ORF2, and GFP-ORF3 constructs was tested in transient expression experiments using PK15 cells. The cells grown in T25 flasks were transfected with GFP vector only, GFP-ORF1, GFP-ORF2, or GFP-ORF3 (2 μg of plasmid per flask) using Lipofectamine Plus (GIBCO/BRL) as described in the manufacturer's protocol. After 24 h posttransfection, the expression of ORF1, ORF2, and ORF3 was demonstrated by immunoblotting analysis using mouse anti-ORF1, anti-ORF2 (J. Liu and J. Kwang, unpublished data), or anti-ORF3 polyclonal antibodies.

RT-PCR. Total cell RNA was prepared from virus-infected PK15 cells by using Trizol RNA extract reagent (Invitrogen) for reverse transcription-PCR (RT-PCR) of the ORF3 gene. The RNA samples were incubated with DNase I for 60 min at 37°C to remove any contaminating viral DNA. The sense primer and the antisense primer were R671 (5′-ATGGTAACCATCCCACCACTTG-3′) and F357 (5′-TTACTGATAGAATGTGGAGC-3′), respectively. The suffix (F or R) of the oligonucleotide indicates the orientation of the primer. F indicates forward direction from nt 0 to 1767, while R indicates reverse direction from nt 1767 to 0. RT-PCR was carried out by using an AMV Reverse Transcriptase kit (Roche) and an Expand High Fidelity PCR kit (Roche), and the PCR product was electrophoresed in 1.2% agarose gel and photographed.
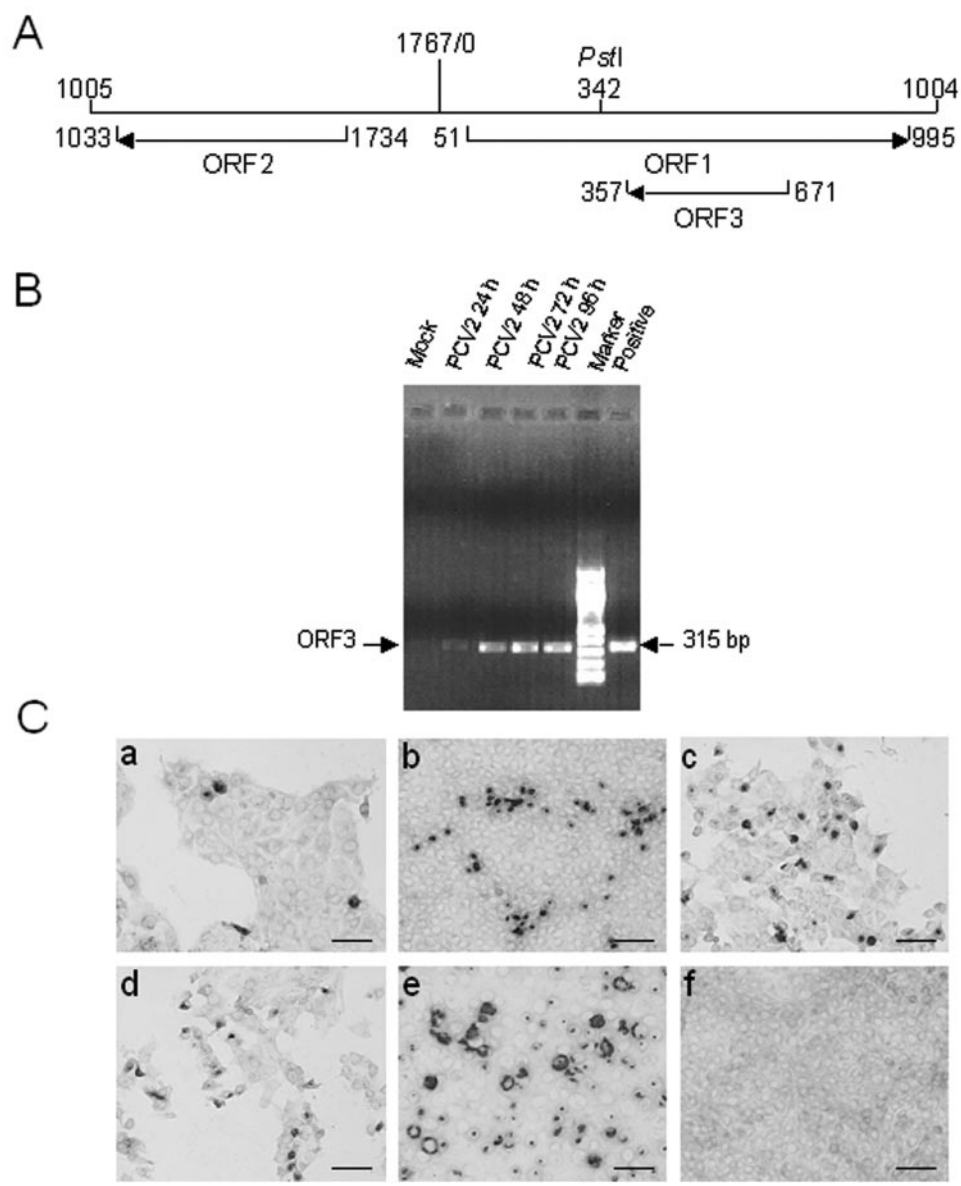
FIG. 1. (A) Genetic map of PCV2 strain BJW (GenBank accession number AY847748). The coding sequences of three open reading frames are annotated with nucleotide coordinates that indicate the nucleotide site of each respective gene. The ORF2 and ORF3 genes are transcribed leftward, and the ORF1 gene is transcribed rightward. The PstI restriction enzyme site is also indicated. (B) Analysis of the ORF3 gene in PCV2-infected cells by RT-PCR. RNA was isolated from PCV2- or mock-infected cells and copied into cDNA. The cDNA was amplified with a pair of ORF3 primers. Positive fragment was amplified from the PCV2 genome using PCR. (C). Detection of ORF3 RNA by ISH from PCV2-infected PK15 cells. ORF3 RNA signals (darkened) were detected in the nucleus of the infected cells at 24 (a), 48 (b), 72 (c), and 96 (d) h postinfection using the antisense ORF3 DIG-labeled riboprobe. The ORF1 RNA signal was also detected in the infected cells at 48 h postinfection using the sense ORF3 riboprobe (e). No signals were detected in the mock-infected cells (f) using the antisense ORF3 riboprobe. Bars, 10 μm.

ISH. In situ hybridization (ISH) was carried out as described below. Briefly, PK15 cells grown in chamber slides (IWAKI) until 80% confluence were infected with wild-type PCV2 or mutant PCV2 at a multiplicity of infection (MOI) of 1 50% tissue culture infective dose (TCID$_{50}$). The slides at 24, 48, 72, and 96 h postinfection were washed with phosphate-buffered saline (PBS), fixed in 4% paraformaldehyde (PFA) solution in PBS for 30 min at room temperature, and dried. After acetylation in a solution of 0.1 M triethanolamine, 0.2 N HCl, and 0.5% acetic anhydride, the slides were prehybridized in hybridization solution (50% formamide, 5× SSC [1× SSC is 0.15 M NaCl plus 0.015 M sodium citrate], 50 μg of salmon sperm DNA/ml) for 2 h at 60°C, followed by overnight hybridization at 60°C with the digoxigenin (DIG)-labeled RNA probes at a concentration of 1 μg/ml. After being washed, the slides were incubated with anti-fluores-cence-AP (Roche) (150 μl of a 1:5,000 dilution in buffer [10% fetal calf serum, 100 mM Tris-HCl, 150 mM NaCl, pH 7.5]) overnight at 4°C. The slides were washed, incubated with Nitro Blue Tetrazolium-BCIP (5-bromo-4-chloro-3-in-dolylphosphate) mixture, and mounted for examination under the microscopy.

The sense riboprobe was synthesized by in vitro transcription with T7 RNA polymerase from pSK plasmid containing the cDNA of ORF3, which was lin-earized with KpnI. For the antisense riboprobe, an ORF3 fragment was ampli-fied using a pair of primers (forward primer, 5′-ATGGTAACCATCCCACCA TTGTTTCTAGGTGGTTTCCAG-3′; reverse primer, 5′-<u>TAATACGACTCAC TATAGG</u>TCAGAAATTTCCGCGGGGCTGG-3′ [T7 promoter underlined]) and transcribed with T7 RNApolymerase. Both RNA probes were labeled by using an NTP-DIG label mix (Roche).

Assay for replication of PCV2. To analyze the growth characteristics of PCV2, confluent PK15 cells were infected with wild-type, recombinant, or mutant PCV2 virus stock (generated after three passages in PK15 cells) at an MOI of 1 $TCID_{50}$. Infected cell cultures were harvested from the cells at different time intervals by three cycles of freeze-thawing followed by clarification. The titer of infectious virus present in the cell culture was determined by IFA on PK15 cells as described previously (14).

Apoptosis assay. PK15 cells grown on chamber slides (IWAKI) at 24, 48, 72, and 96 h postinfection were fixed with 4% PFA in PBS and stained with porcine anti-PCV2 serum and fluorescein isothiocyanate-conjugated antibody. For transfection, transfected PK15 or Cos-7 cells with GFP-ORF1, GFP-ORF2, or GFP-ORF3 plasmid were fixed with 4% PFA at 24 and 48 h posttransfection, respectively. The slides were then incubated with DAPI (2,4-diamidino-2-phenylindole) at a concentration of 1 μg/ml for 30 min at 37°C and examined under an LSM 510 META confocal laser scanning microscope (Zeiss, Germany) with a Plan-Novofluar 63×/1.4 oil objective.

Infected PK15 cells (2×10^6 to 3×10^6) at different intervals postinfection were scraped and centrifuged at $1,000 \times g$ for 10 min at 4°C. Pellets were washed in PBS and fixed in 2.5% glutaraldehyde. Subsequently, the cells were postfixed in 1% OsO_4 and embedded in Epon 812. Ultrathin sections were cut and examined under a Hitachi H-700 electron microscope.

PK15 cells grown in T75 flasks were infected with wild-type PCV2. Following treatment, floating and trypsin-detached cells were pooled and washed twice with ice-cold PBS and fixed in 70% cold ethanol and then washed twice in PBS. After centrifugation, the cell pellets were stained PBS-propidium iodide (50 μg/ml) and RNase A (100 μg/ml) for 45 min. DNA content of PK15 cells was analyzed by fluorescence-activated cell sorting (FACSort; Becton Dickinson). At least 10,000 events were analyzed, and the percentage of cell in the sub-G_1 population was calculated. Aggregates of cell debris at the origin of the histogram were excluded from the analysis of sub-G_1 cells. In each experiment, mock-infected PK15 cells were used as controls and compared with cells infected with PCV2.

Adherent and nonadherent cells from infected cells with wild-type PCV2 or transfected cells with GFP-ORF1, GFP-ORF2, or GFP-ORF3 plasmid were collected separately, sedimented at $200 \times g$ for 10 min, washed with ice-cold PBS, fixed in 4% PFA, stained with 1 μg/ml DAPI, and examined by florescence microscopy. A minimum of 300 cells/sample were scored for apoptotic changes (fragmentation of the nucleus into multiple discrete fragments).

Fluorimetric assay of caspase activity. Spectrofluorometric assays of proteolytic activity were carried out using synthetic fluorogenic substrates 7-amino-4-trifluoromethyl coumarin (AFC) to measure caspase-8 or caspase-3 activity and 7-amino-methyl coumarin (AMC) to measure caspase-9 activity. BD ApoAlert caspase fluorescent assay kits (Clontech Laboratories) were used to determine caspase-3, caspase-8, and caspase-9 activities. In brief, 80% confluent monolayers of PK15 cells grown in 25 25-mm flasks were infected wild-type PCV2 or mutant PCV2 or were transfected with 2 μg of GFP-ORF1, GFP-ORF2, GFP-ORF3, or GFP vector alone. After infection/transfection, cells were harvested at $400 \times g$ for 5 min. Cells (2×10^6 to 3×10^6) were lysed in 50 μl of lysis buffer on ice for 10 min and centrifuged at $16,000 \times g$ for 10 min, and the supernatant was collected. Fifty microliters of supernatant was added to an equal volume of 2× reaction/dithiothreitol buffer supplemented with caspase-3 substrate DEVD-AFC (50 μM), caspase-8 substrate IETD-AFC (50 μM), or caspase-9 substrate LEHD-AMC (250 μM) and incubated at 37°C for 2 h. The optical densities for caspase-3, caspase-8, and caspase-9 were determined at 405 nm. The nanomoles of AFC or AMC released per hour were calculated from the standard curve.

IFA. For infection, PK15 cells grown on the chamber slides (IWAKI) were incubated with wild-type, recombinant, or mutant PCV2 for 60 min at 37°C at an MOI of 1 $TCID_{50}$ and added to minimal essential medium for incubation. Following the incubation at 37°C, cells at 24, 48, 72, and 96 h postinfection were washed with PBS and fixed for 30 min at room temperature with 4% PFA in PBS. After fixation, the cells were blocked by PBS-Tween (PBS-T) with 3% bovine serum albumin (BSA) at room temperature for 1 h. Primary antibody, mouse anti-ORF3 polyclonal antibodies, or porcine anti-PCV2 antibody was diluted in PBS-T with 1% BSA and incubated with the cells for 1 h at 37°C. After washing with PBS, the cells were incubated with rabbit anti-mouse or anti-porcine fluorescein isothiocyanate-conjugated antibody (Sigma) diluted in PBS-T with 1% BSA for 1 h at 37°C. The cells were washed three times with PBS, rinsed in distilled water, dried, and mounted with fluorescence mounting medium and examined using fluorescence microscopy.

Western blot analysis. The whole-cell lysates from wild-type PCV2-infected PK15 cells were resolved by 15% sodium dodecyl sulfate-polyacrylamide gel electrophoresis (SDS-PAGE) and blotted onto nitrocellulose membranes (Stratagene) with a semidry transfer cell (Bio-Rad Trans-Blot SD). The membranes were blocked for 2 h at room temperature in blocking buffer TBST (20 mM Tris-HCl [pH 7.4], 150 mM NaCl, 0.1% Tween 20) containing 5% skim milk powder to prevent nonspecific binding and then incubated with mouse anti-ORF3 antibody at room temperature for 2 h. The membranes were then washed three times with TBST and incubated for 1 h at room temperature with horseradish peroxidase-conjugated anti-mouse secondary antibody (DAKO) diluted in blocking buffer (1:2,000). After washing, the membrane was reacted with 3,3′-diaminobenzidine tetrahydrochloride (Pierce, Rockford, Ill.) substrate (20 ml [0.1 M Tris-HCl {pH 7.4], 20 mg DAB {3,3′-diaminobenzidine tetrahydrochloride}, and 6.8 μl H_2O_2]) and then stopped with distilled water.

Nucleotide sequence accession number. The genome sequence of PCV2 strain BJW has been deposited in GenBank under accession number AY847748.

RESULTS

Identification of a novel viral protein, ORF3, in PCV2-infected cells. The whole-cell nucleic acid of infected and mock-infected PK15 cells was analyzed by RT-PCR. Amplification products were separated by agarose gel electrophoresis (Fig. 1B). A 315-bp fragment, the ORF3 gene, was amplified by using RNA isolated from PCV2-infected cells at the times indicated, suggesting that the ORF3 gene could express at the level of transcription in the PCV2-infected cells. PCV2-infected PK15 cells were further analyzed to determine the relative distribution of the ORF3 mRNA. As shown in Fig. 1C (panels a to d), the signals of ORF3 mRNA were detected in PCV2-infected cells at the time indicated using the antisense riboprobe as expected and located predominantly in the nucleus of the infected cells. Interestingly, the mRNA signals were also detected in the infected cells (Fig. 1C, panel e) by using the sense ORF3 riboprobe, and they were ORF1 mRNA in that the full ORF3 gene is completely overlapping the ORF1 gene at the counterdirection in the PCV2 whole genome (Fig. 1A). In addition, no signals were detected in control cells without PCV2 infection (Fig. 1C, panel f). The results further indicated that the ORF3 mRNA could be detected in PCV2-infected cells and located in the nucleus.

The ORF3 gene was cloned into *E. coli* vector PQE30 and expressed (data not shown). This recombinant protein was further confirmed by Western blotting using anti-histidine monoclonal antibody (data not shown) and could be prepared for production of monospecific antibody against the protein ORF3, which was used in the following experiments.

To determine whether ORF3 protein was expressed in PCV2-infected PK15 cells, cells were infected with PCV2 (strain BJW) as described in Materials and Methods. Anti-ORF3 mouse polyclonal antibody was used in direct immunofluorescence experiments to determine the expression and localization of ORF3 in PCV2-infected PK15 cells. Clusters of cells expressing ORF3 can be detected in cells that have been infected with PCV2 at 24, 48, 72, and 96 h (Fig. 2A, panels b to d, and data not shown) postinfection. The ORF3 protein was located predominantly in the nucleus and to a lesser degree in the cytoplasm of the infected cells. As shown in Fig. 2A (panel c), the ORF3 protein was maximally expressed in the infected cells at 48 h postinfection. No significant staining was observed in mock-infected cells (Fig. 2A, panel a), indicating the specificity of the mouse antibody against ORF3. Total proteins were further harvested from PK15 cells at the times indicated postinfection and subjected to Western blotting (Fig. 2B). By using the mouse anti-ORF3 antibody, the protein was detected in PCV2-infected cells at 24 h postinfection as a faint but clearly discernible signal. The intensity of the bands in-
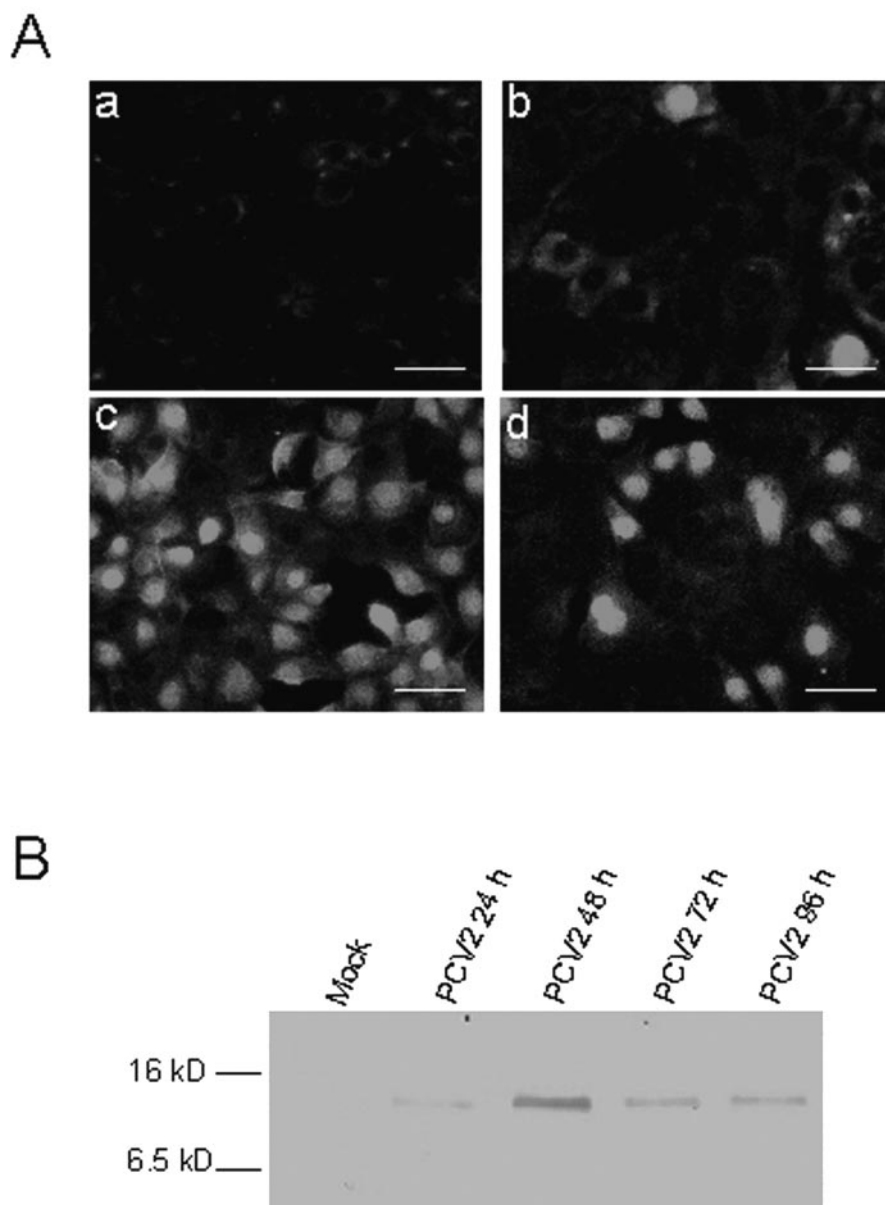
A

B

FIG. 2. Expression of ORF3 protein in PCV2-infected cells. (A) PCV2-infected PK15 cells were probed with antiserum raised against the ORF3 protein of PCV2. IFA staining of PK15 cells after infection with PCV2 strain BJW at 24 (b), 48 (c), and 72 (d) h postinfection is shown. Panel a was used as a negative control when mock-infected PK15 cells were stained by IFA. The cells were visualized and photographed using fluorescence microscopy. ORF3 antigen was located in the nucleus and to a lesser degree in the cytoplasm of the infected cells. Bars, 10 μm. (B) Total cell lysates from the PCV2 strain BJW-infected PK15 cells were electrophoresed by 15% SDS-PAGE, transferred onto nitrocellulose membrane, and detected by antiserum against ORF3 antibody. ORF3 protein was expressed in the PCV2-infected cells after infection.

creased considerably thereafter but decreased at 72 h postinfection. No signal was detected in mock-infected cells (Fig. 2B).

Together, these results show that ORF3 is considered a novel viral protein due to its expression at both transcription and translation levels in PCV2-infected cells.

ORF3 is not essential for viral replication. As described in Materials and Methods, the ORF3 gene was deleted by a mutation of the start codon from ATG to GTG to generate a PCV2 mutant lacking ORF3. To study the function of the ORF3 protein in viral replication, PK15 cells were transfected with wild-type PCV2 or mutant PCV2 infectious clone DNA. While wild-type PCV2 DNA generated rPCV2 as expected, the PK15 cells transfected with the mutant PCV2 DNA also generated a viable mutant virus (rPCV2ORF3Δ). The mutant virus was passaged three times in PK15 cells to increase virus titers. Thereafter, the whole-cell nucleic acid of infected and mock-infected cells was analyzed by RT-PCR. Reaction products were separated by agarose gel electrophoresis (data not shown). A 315-bp fragment was amplified by using RNA isolated from the mutant PCV2-infected cells as seen in the wild-type PCV2-infected cells, indicating that a point mutation oc-
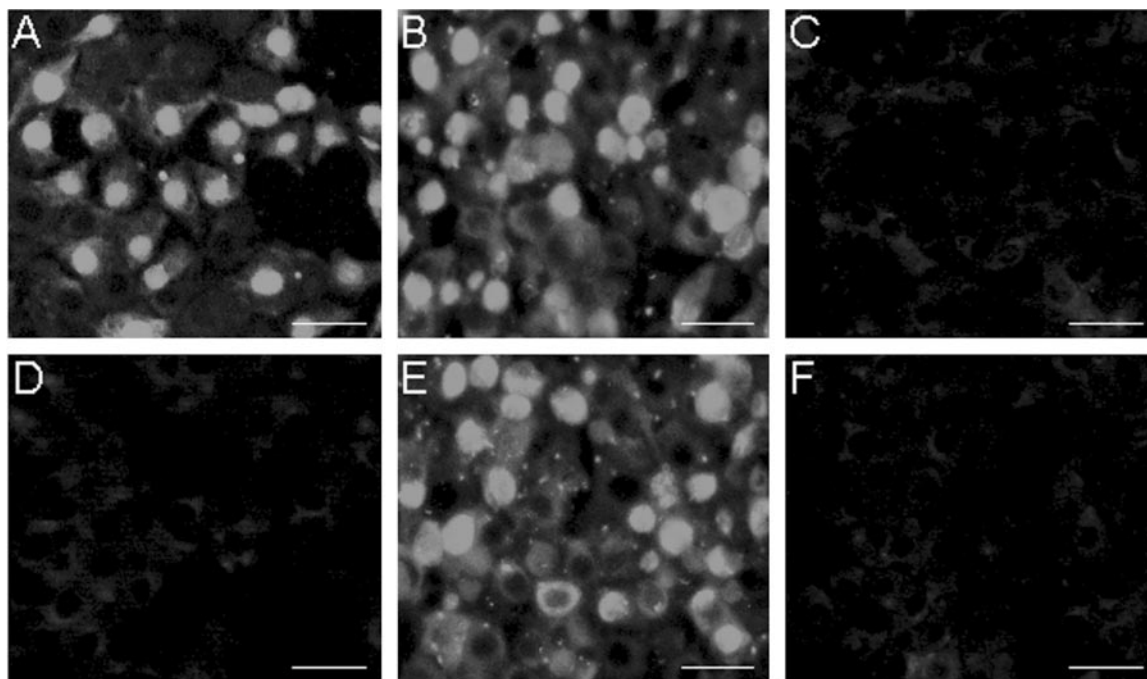
FIG. 3. IFA staining of ORF3-deficient PCV2-infected cells used to detect ORF3 protein expression. PK15 cells were infected with recombinant PCV2 virus stock (A and B) or with passage 5 of the ORF3-deficient PCV2 virus stock (D and E) at an MOI of 1. Mock-infected PK15 cells were used as negative controls (C and F). At 48 h postinfection, the cells were fixed and analyzed by immunofluorescence staining with mouse anti-ORF3 serum (A, D, and F) or porcine anti-PCV2 serum (B, C, and E). Bars, 10 μm.

curring in the start codon of the ORF3 gene did not affect its transcription and further suggesting that the start site of ORF3 transcription may locate upstream. No PCR product was obtained using mock-infected PK15 cells. Sequence analysis of the RT-PCR products confirmed the presence of the desired alteration in the generated PCV2 mutant (data not shown). In addition, mRNA signals of the ORF3 gene were detected in the nucleus of mutant PCV2-infected cells by using the antisense ORF3 riboprobe (data not shown).

To detect the expression of the ORF3 protein, PK15 cells were infected with the recovered viruses and analyzed by IFA using ORF3-specific antiserum. Figure 3 shows the results of immunofluorescence staining of recombinant or mutant PCV2-infected cells. Cells infected with rPCV2 virus expressed ORF3 protein and gave a positive immunofluorescence signal (Fig. 3A). However, cells infected with mutant rPCV2ORF3Δ virus failed to give any fluorescence signal (Fig. 3D), indicating the absence of ORF3 protein expression, even after passage 12 (data not shown). In contrast, anti-PCV2 porcine serum readily detected viral antigens in the nucleus of recombinant as well as mutant PCV2-infected cells (Fig. 3B and E). No fluorescence was detected in the mock-infected cells using anti-ORF3 mouse serum (Fig. 3F) or anti-PCV2 porcine serum (Fig. 3C).

To determine the replication kinetic of wild-type, recombinant, and ORF3-deficient PCV2, PK15 cells were infected with each virus, and the virus titer was determined by IFA assay at 5 days after infection. Figure 4A depicts the growth curve of each virus (expressed as $TCID_{50}$/milliliter) at different times postinfection. The $TCID_{50}$ at the different time points after infection showed that the mutant virus (lacking the expression

of ORF3 protein) replicated somewhat more slowly than the parent virus PCV2 or recovered rPCV2 virus. At 36 h after infection, the ORF3-deficient PCV2 virus showed a titer approximately 33- or 31-fold lower than that of the parent virus PCV2 or recovered rPCV2 virus, respectively. However, at 72 h postinfection, the ORF3-deficient PCV2 virus reached a titer of $10^{5.5}$ $TCID_{50}$/ml, which was similar to those of the parent virus PCV2 ($10^{5.8}$ $TCID_{50}$/ml) and recovered rPCV2 virus ($10^{5.6}$ $TCID_{50}$/ml). These results indicate that the ORF3 protein is not required for replication in cell culture.

PCV2 infection induces apoptosis in cultured cells through the caspase-8 pathway. PCV2 replication in PK15 cells during the late stage of infection resulted in cytopathic effects such as rounding up, detachment of infected cells from the culture flask, and cell lysis and death. The mechanisms that lead to the death of PCV2-infected cells are not fully understood. To determine whether PCV2 infection induced apoptosis in cultured cells, we inoculated PK15 cells with wild-type PCV2 at an MOI of 1 $TCID_{50}$ and analyzed them for PCV2 viral antigen expression by IFA and apoptosis by DAPI staining at different times postinfection. Intact nuclei are stained evenly, but apoptotic nuclei are often fragmented and show irregular or weak DNA staining caused by condensation and fragmentation of the DNA (45). Figure 5A shows that chromatin condensation and fragmentation were visible in the PCV2-infected cells at 48 h (upper panel) and 72 h (lower panel) postinfection. In contrast, no obvious nuclear morphological changes were observed in mock-infected cells after infection (data not shown).

Infected and mock-infected PK15 cells were analyzed for their ultrastructural features. At 48 h postinfection, the cells infected with PCV2 showed features typical of programmed
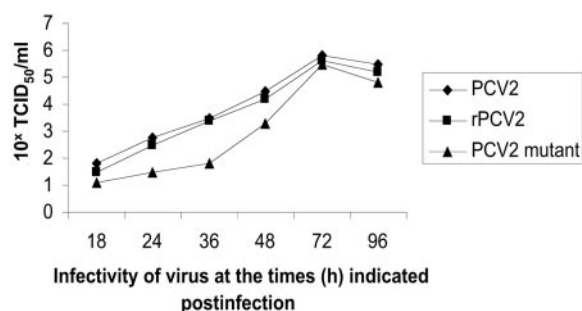
FIG. 4. Replication kinetics of ORF3-deficient PCV2 as well as recombinant PCV2 and wild-type PCV2. PK15 cells were infected with the indicated viruses at an MOI of 1 and harvested at the indicated time points, and infectious titers in $TCID_{50}$ per milliter were determined by IFA. "$10\times$" denotes 10 times the value on the *y* axis.

cell death, such as changes in the density and distribution of chromatin, which condensed peripherally into a crescent-shaped mass, and dilatation of nuclear cisternae were observed (Fig. 5B, panel b). At 72 h postinfection, cells displayed the typical markers of apoptotic cell death such as nuclear segmentation and cytoplasmic derangement, which are responsible for the formation of apoptotic bodies (Fig. 5B, panel c). At 96 h, cells exhibited further nuclear fragmentation, leading to extensive dispersion of apoptotic bodies (data not shown). In contrast, the mock-infected cells did not display detectable alterations at the ultrastructural level (Fig. 5B, panel a).

The PCV2-induced apoptosis was assessed by determining the proportion of hypodiploid cells by flow cytometry of propidium iodide-stained, fixed PK15 cells. Apoptotic cells have a lower DNA content than normal cells, and their presence is distinguished by the appearance of a hypodiploid peak of lower fluorescence. For mock-infected cells, ~1% of cells were hypodiploid based on fluorescence-activated cell sorting analysis of propidium iodide-stained cells (Fig. 6A), whereas the hypodiploid cells that increased significantly at 72 h postinfection subsequently decreased (Fig. 6A and data not shown). Induction of apoptosis by PCV2 was also scored by analysis of nuclear morphology by DAPI staining as described in Materials and Methods. Examination of stained cells demonstrated that apoptotic cells showed in a similar manner (Fig. 6B) after infection as described in the flow cytometry analysis. As shown in Fig. 6C, more cells detached from the culture flask and entered into the substratum in the inoculate cultures than in the mock-inoculated cultures.

The effector phase of apoptosis requires the activation of several caspases (11, 31). To determine which caspases are involved in PCV2-induced apoptosis, synthetic fluorogenic substrate AFC was used to measure caspase-8 and caspase-3 activity or AMC was used to measure caspase-9 activity. Cleavage of these substrates by cytoplasmic extracts is indicative of the proteolytic activation of these caspases in response to PCV2-induced apoptotic signals. Following infection with PCV2, there was a time-dependent increase in the level of DEVD-AFC cleavage at 72 h postinfection which decreased abruptly thereafter (Fig. 7), indicating that caspase-3 was progressively activated. In addition, when PCV2-infected cells were treated with acetyl-DEVD-CHO, a peptide inhibitor of caspase-3 activity, blockage in PCV2-induced apoptosis was

observed (Fig. 7). As in caspase-3, fluorescence assay using a specific fluorogenic peptide (IETD-AFC) showed that caspase-8 was activated in a similar time-dependent manner after infection with PCV2 (Fig. 7). A similar experiment was performed using a caspase-8 inhibitor, IETD-fmk, and no caspase-8 activity was detected in PCV2-infected cells (Fig. 7). The role of the caspase-9 pathway in the induction of apoptosis was investigated by using substrate LEHD-AMC after infection with PCV2 (Fig. 7). This indicates that the level of caspase-9 activity in infected PK15 cells remained stable and similar to those in mock-infected cells or infected cells treated with LEHD-CHO (a specific caspase-9 inhibitor) during the infection. Thus, the results indicate that PCV2 induced apoptosis in cultured cells through activation of the initiator caspase-8 followed by activation of the effector caspase-3 pathway; the initiator caspase-9 is not involved in the process of initiation of apoptosis in PK15 cells.

ORF3 protein alone induces apoptosis involving the caspase-8 pathway. After confirming that PCV2 infection induces apoptosis in PK15 cells, the permissive cell line for PCV2 infection, we then tried to screen for PCV2-encoded proteins (virus-encoded proapoptotic proteins) that may be responsible for the induction of apoptosis. The ORF1, ORF2, and ORF3 genes were cloned into a mammalian expression vector, pEGFP-C1, under the control of the human cytomegalovirus promoter. The PK15 and Cos-7 cells were transfected with these plasmids, and the expression of each protein was directly examined by fluorescence microscopy and further confirmed by immunoblotting analysis using mouse anti-ORF1, anti-ORF2, or anti-ORF3 antibody (data not shown). The protein ORF1, ORF2, or ORF3 was localized to the transfected nucleus region similar to that seen in infected cells (data not shown). After transfection of cells with individual constructs, the cells were stained with DAPI at 24 and 48 h posttransfection. As shown in Fig. 8A, chromatin condensation and fragmentation, which are typical features of apoptosis, were seen in the ORF3-expressing PK15 cells (upper panel) and Cos-7 cells (lower panel) by nuclear DAPI staining at 24 h posttransfection. In contrast, no obvious nuclear morphological changes were observed in ORF1- or ORF2-transfected cells (data not shown). Furthermore, the total GFP-positive cells and the number of cells with fragmented or condensed nuclei among the GFP-positive cells were counted, and the percentage of dead cells was calculated. As shown in Fig. 8B, expression of the ORF3 protein as GFP fusion constructs in transfected PK15 cells induced 10% and 25% of dead cells at 24 and 48 h posttransfection, respectively. ORF3 also caused 12% and 28% of dead cells at the time points when transfected into Cos-7 cells (data not shown). Expression of ORF1 and ORF2 proteins did not lead to significantly more dead cells than what was seen in the control in this screening, regardless of transfected PK15 (Fig. 8B) or Cos-7 cells (data not shown). In contrast, GFP alone could induce less than 4% of dead cells when transfected into both PK15 and Cos-7 cells at time points posttransfection (Fig. 8B and data not shown). Furthermore, more cells detached from the culture flask and entered into the substratum in the ORF3-transfected PK15 (Fig. 8C) and Cos-7 cells (data not shown) than in the transfection control using GFP alone as well as ORF1- or ORF2-transfected cells (Fig. 8C and data not shown).
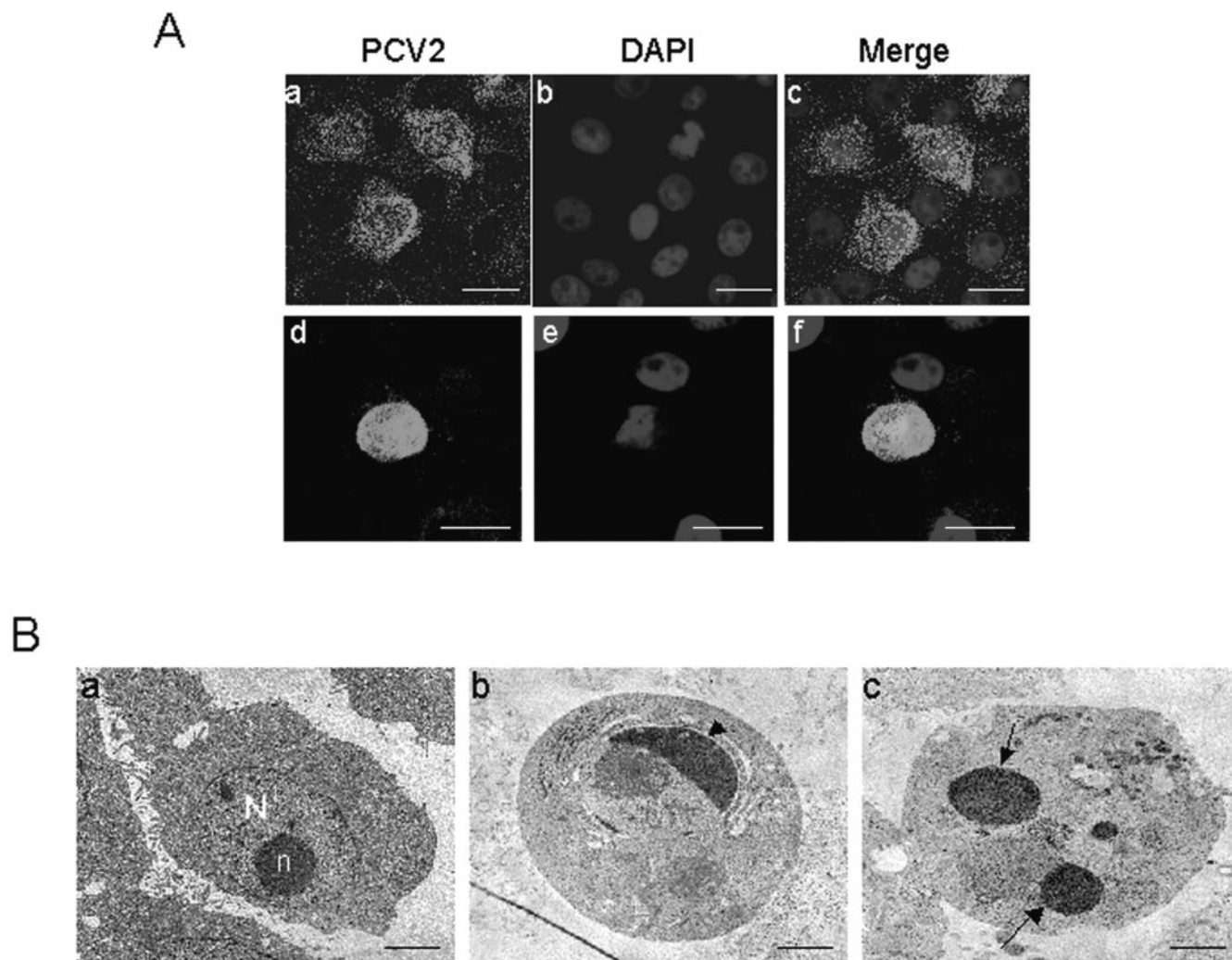
FIG. 5. PCV2 induces apoptosis in cultured PK15 cells. (A) PCV2-infected PK15 cells showed nucleosomal DNA fragmentation by DAPI staining. Cells infected with the PCV2 strain BJW at 48 (a and b) and 72 (d and e) h postinfection were detected by IFA using porcine serum against PCV2 and stained with DAPI, respectively. Overlaid images are shown in c and f. Bar, 10 μm. (B) Apoptosois induced by PCV2 is observed under an electron microscope. In a mock-infected cell (a), the complete nucleus (N) displays a large, unique, electron-dense nucleolus (n). Cells at 48 (b) and 72 (c) h postinfection display typical markers of apoptosis such as chromatin condensed peripherally into a crescent-shaped mass (short arrow) and nuclear fragmentation, which forms apoptotic bodies. Bars, 2 μm.

Caspase-8 and caspase-3 have been implicated in apoptosis induced by PCV2 in permissive PK15 cells as demonstrated above. We examined caspase-3, caspase-8, and caspase-9 activation in the ORF3-transfected PK15 cells using fluorometric caspase assay as described in Materials and Methods. Caspase-8 and caspase-3 are activated in a time-dependent manner in transfected cells and blocked by the addition of IETD-fmk and acetyl-DEVD-CHO (Fig. 9A and B), respectively. In contrast, the ORF3-transfected cells could not produce any obvious caspase-9 activity (Fig. 9B) compared to that in the transfected cells with GFP alone. In addition, ORF1 and ORF2 could not trigger caspase activity in transfected PK15 cells in this study (Fig. 9A and data not shown). The results suggest that the ORF3 protein alone induces apoptosis in transfected cells by activating caspase-8 and caspase-3 pathways similar to that described in the context of PCV2 infection.

To determine the apoptotic effects of rPCV2ORF3Δ in PK15 cells, the cells were infected with the mutant virus at an MOI of 1 $TCID_{50}$, harvested at different time intervals, and analyzed by caspase-3 activity. Apoptotic activity induced by the mutant virus was significantly lower than that produced by wild-type PCV2 virus after infection (Fig. 9C). No appreciable level of apoptosis was detected in the mock-infected cells (Fig. 9C). This result indicates that PCV2-induced cell death is significantly reduced due to the absence of ORF3 protein expression.

DISCUSSION

Two major open reading frames have been identified within the genome of PCV. The *cap* gene ORF2 encodes viral capsid, the major structural protein. The other gene, *rep* (ORF1), directs the synthesis of the two *Rep* isoforms, *Rep* and *Rep'*, which are essential for viral replication (9, 25). In addition, six
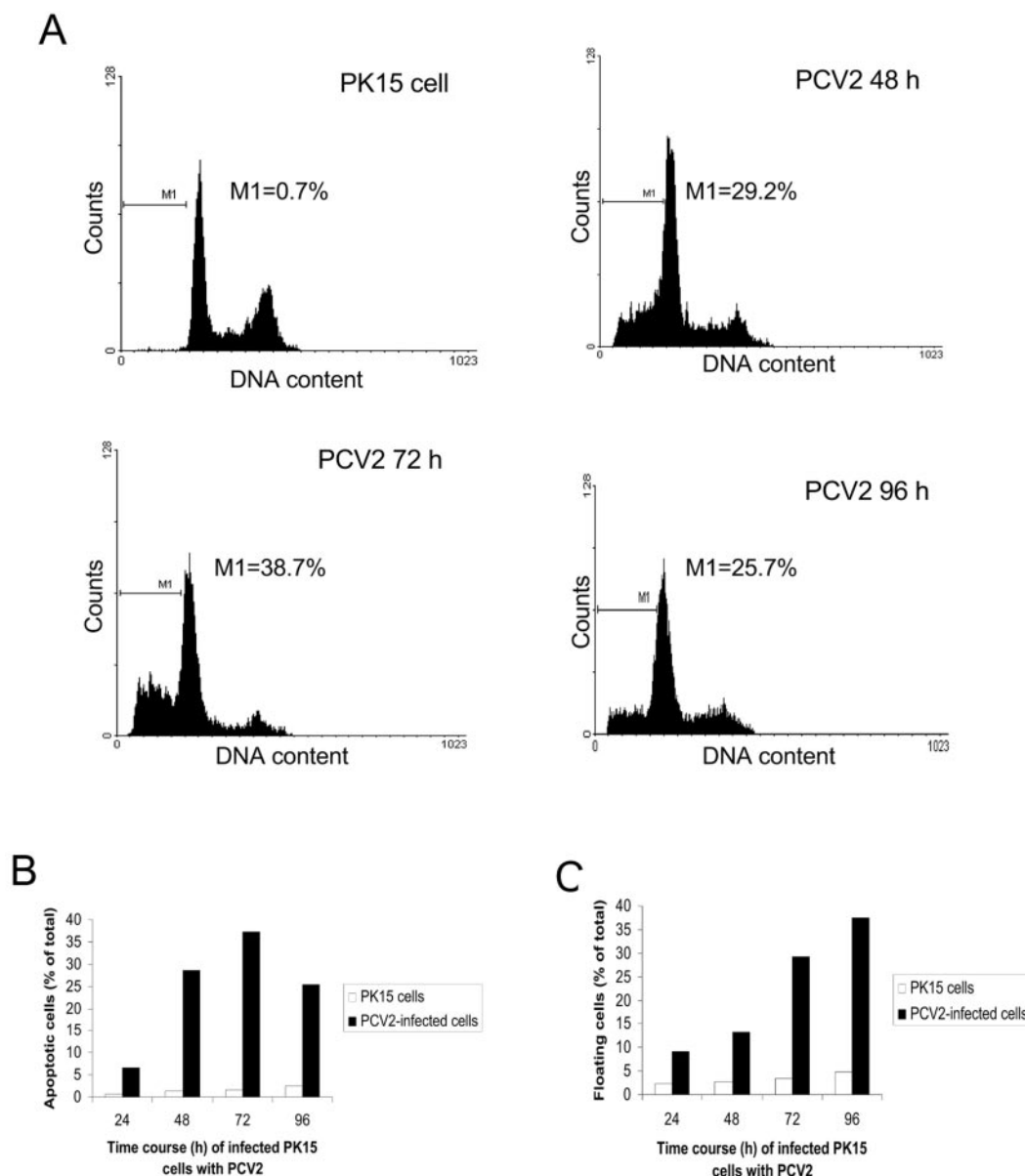
FIG. 6. PCV2-induced apoptotic cells were quantitatively determined. (A) Representative figures of the determination of apoptosis by propidium iodide staining and flow cytometry of PK15 cells infected with PCV2 strain BJW. For each panel, the percentage of PK15 cells with hypodiploid (apoptotic) DNA content is indicated (M1). B shows the average percentage of apoptosis of three experiments shown in A. C shows the average percentage of detached cells of three experiments at the times indicated.

more RNAs (three *Rep*-associated RNAs, *Rep3a*, *Rep3b*, and *Rep3c*, and three NS-associated RNAs, NS515, NS672, and NS0) of PCV2 were detected during productive infection in porcine kidney cells (9, 10), suggesting that these transcription units did not have any effect on viral protein synthesis or DNA replication. NS515, NS672, and NS0 have been considered to be transcribed from three different promoters inside ORF1 downstream of the *Rep* promoter (9) and might not code for any proteins or functional proteins. Among the nine PCV2-specific RNAs identified, only ORF2 RNA is transcribed from the cDNA strand and encodes the viral capsid protein ORF2. In the present study, we have detected a novel viral RNA

transcribed from the cDNA strand of the genome in PCV2-infected PK15 cells and further demonstrated that it encodes a novel viral protein (termed ORF3 here) which is involved in PCV2-induced apoptosis in cultured cells.

In this study, a novel transcript ORF3 RNA was readily detected by RT-PCR in PCV2-infected cells (Fig. 1B) and further detected in the nucleus of the infected cells by using ISH assay (Fig. 1C). Furthermore, using specific antibody against the ORF3 protein, we have shown by immunofluores-cence that the protein is expressed in PK15 cells infected with PCV2 (Fig. 2A) and is predominantly located in the nucleus of the infected cells and to a lesser degree in the cytoplasm (Fig.
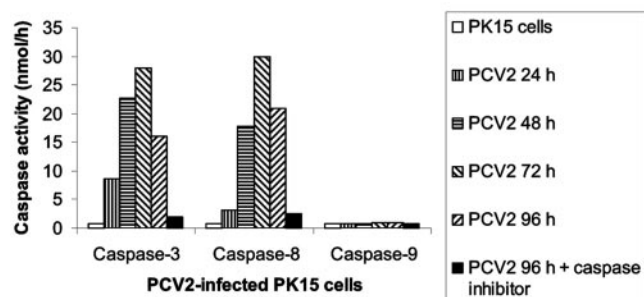
FIG. 7. Apoptosis induced by PCV2 is dependent on caspase-3 and caspase-8 activity but not on caspase-9 activity. Cell lysates were harvested at the indicated time points postinfection and assayed for DEVDase, IETDase, or LEHDase activity using specific substrate DEVD-AFC (caspase-3), IETD-AFC (caspase-8), or LEHD-AMC (caspase-9), respectively. Simultaneously, the cells at 96 h postinfection were treated with inhibitor DEVD-CHO (for caspase-3), IETD-fmk (for caspase-8), or LEHD-CHO (for caspase-9), respectively. In all of the above-mentioned caspase activity assays, mock-infected cells were used as a negative control for each of the infections. While caspase-3 or caspase-8 activity increases up to 72 h postinfection and then abruptly declines, the level of caspase-9 activity in infected cells remains stable and similar to that in mock-infected cells. In addition, in the absence of infection, the inhibitors did not demonstrate any effects on apoptosis. Values shown are means from duplicated experiments.

2A). The protein expression in the infected cells could also be detected by Western blot analysis (Fig. 2B). Analysis of the sequences of over 20 different geographic PCV2 isolates (obtained from the GenBank database) suggested that the ORF3 protein is highly conserved in PCV2 strains studied, with greater than 94.5% identity at the amino acid level (data not shown). However, the corresponding region of PCV1 strains appears to be different and shows only 61.5% amino acid sequence identity. Since PCV1 viruses are naturally nonpathogenic and do not cause any pathological lesions in pigs (3, 48), these residues may play a role in the pathogenicity of the virus.

In the absence of ORF3, in vitro replication of PCV2 is delayed (Fig. 4). However, the maximal titer is as high as those found after wild-type virus replication. It will be interesting to analyze the growth behavior of mutant PCV2 in pigs, the natural host of PCV2. It is conceivable that the delay in replication translates into attenuation in vivo, leading to a virus strain with vaccine potential. For PCV2, ORF2 protein has been considered as a major immunogenic capsid protein (9, 30, 31) and could stimulate a protective response in pigs inoculated with baculovirus-expressed recombinant ORF2 (5) or injected with DNA vaccine from ORF2 (5, 19). Chimeric PCV1-2 virus with the ORF2 gene of PCV2 cloned into the nonpathogenic PCV1 genomic backbone could also induce a strong immune response against PCV2 while it is mildly pathogenic (15), suggesting that the ORF2 protein of PCV2 is a good host-protective immunogen. The immunodominant epitopes of the ORF2 protein have been further shown to likely locate within amino acid residues 47 to 84 and 165 to 200 and the last four amino acids of the protein (22). These indicate that the antibody induced by the ORF3 protein might not be involved in the protective immune response of the host. Also, the PCV2 mutant lacking the ORF3 protein could result in the failure to induce corresponding antibody in the animal and could be

expected to elicit an appropriate immune response as wild-type PCV2. Whether this approach will eventually lead to a novel marked vaccine against PCV2 infection remains to be determined in vivo.

Virus-induced cell death plays an important role in the pathogenesis of virus infection. Apoptosis may represent an important step in the spread of progeny to neighboring cells while evading the host immune system (46) and function by eliminating aberrant cells created by DNA damage or those infected by viral pathogens (39). Many viruses have been demonstrated to elicit or inhibit apoptosis either directly or indirectly during their replication cycles (39). In the *Circoviridae* family, chicken anemia virus (CAV) induced apoptosis in thymocytes and cell lines after infection (18), and the VP3 protein, apoptin, encoded by CAV triggered apoptosis in various cultured transformed cell lines (34). For PCV2, it has been shown to induce apoptosis in B lymphocytes of affected swine followed by selective B-lymphocyte depletion (43) and has also been shown to trigger apoptosis in histiocytic cells in lymphoid tissues in a mouse model of PCV2 infection (21). However, contrary results have recently been reported that show that lymphocyte apoptosis is not significantly induced and that caspase-3 activity was not significantly stimulated in naturally affected pigs compared to normal controls (24, 37), which suggested that lymphoid tissue depletion was related mainly to decreased proliferative activity in lymphoid tissue. However, here, we have demonstrated that PCV2 was capable of inducing apoptosis in the cultured PK15 cells by using DAPI staining, electron microscopic observation, and flow cytometric analysis. The DAPI staining showed irregular or weak DNA staining (Fig. 5A) caused by condensation and fragmentation of the DNA (45), which is consistent with the morphological changes under electron microscopic observation, including extensive chromatin condensation and appearance of apoptotic bodies (Fig. 5B). Apoptotic cells (Fig. 6B) determined by evaluation of the DAPI staining and hypodiploid cells (Fig. 6A) analyzed by flow cytometry significantly increased compared to the mock-infected controls after PCV2 infection. The cells detached and floated into the substratum by up to 40% after infection with PCV2, whereas the floating cells in the mock-infected control were less than 5% (Fig. 6C). By expressing individual viral proteins in a cultured cell line, we provided further evidence that a novel viral protein encoded by the ORF3 gene contributes to the induction of apoptosis during PCV2 infection.

In this study, we further investigated the mechanism by which PCV2 induces the apoptosis of the cultured PK15 cells. We found that PCV2-induced apoptosis seems to be caspase dependent, based on its activation of caspase-8 and caspase-3 in the execution of the apoptotic process. Caspases are the central players in apoptosis. At least two major pathways for caspase activation have been delineated, including an extrinsic pathway linked to the tumor necrosis factor family of death receptors and an intrinsic pathway activated by mitochondria. The apical proteases in the extrinsic and intrinsic pathways are caspase-8 and caspase-9, respectively (40). No obvious increase in LEHD-AMC activity of the PCV2-infected cells was noted compared to that of the mock-infected cells, whereas the results of high activity of IETD-AFC which can be inhibited by IETD-CHO in the PCV2-infected cells suggested that PCV2
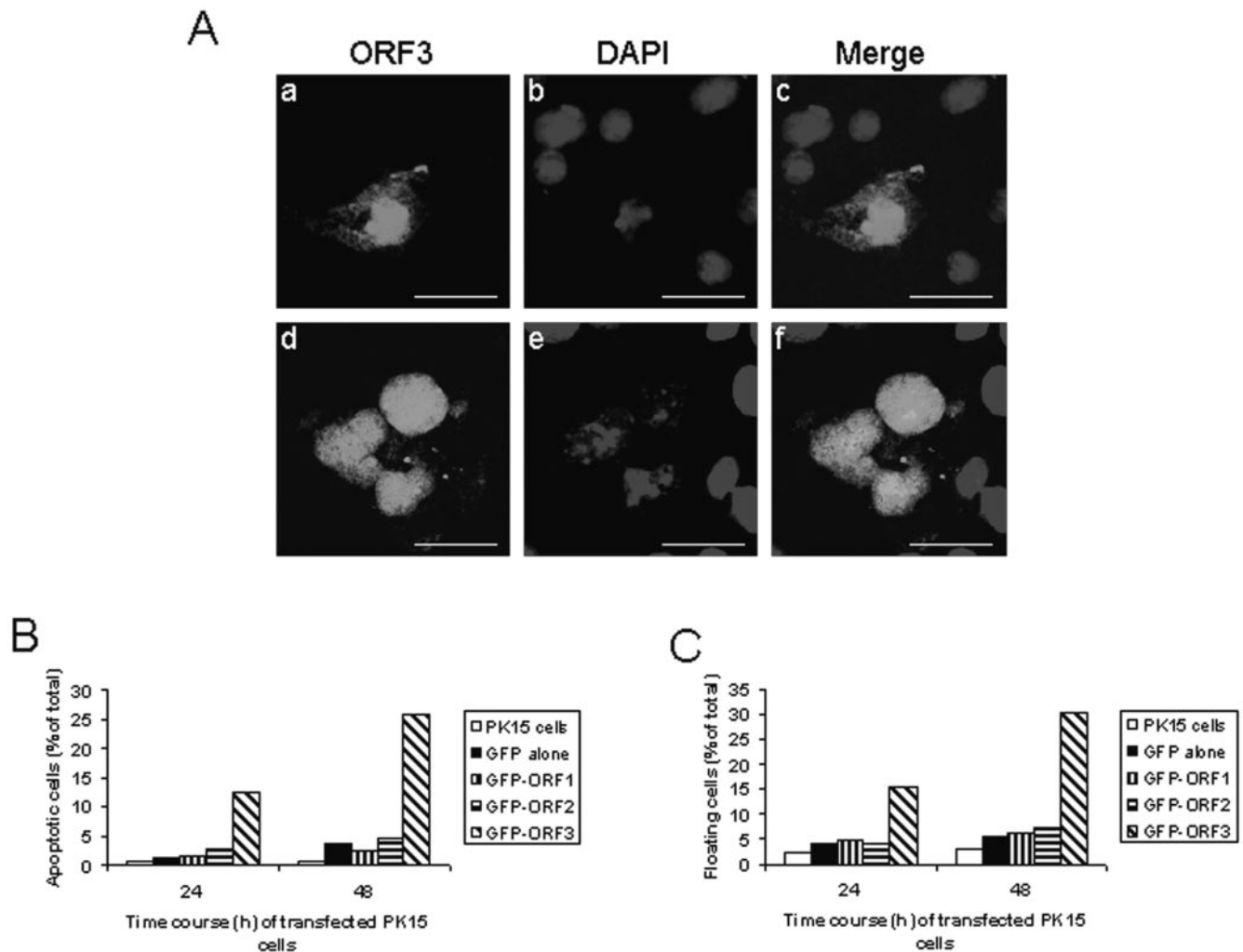
FIG. 8. ORF3 protein alone induces apoptosis in transfected cells. (A) PK15 and Cos-7 cells transfected with GFP-ORF3 plasmid at 24 h showed ORF3 expression (a and d) and nucleosomal DNA fragmentation (b and e) by DAPI staining, respectively. Overlaid images are shown in c and f. Bar, 10 mm. (B) Quantitative analysis of apoptosis induced by the ORF3 protein. The average percentage of apoptotic cells of three experiments was scored by analysis of nuclear morphology by DAPI staining as described in Materials and Methods. Panel C shows the average percentage of detached cells of the three experiments as shown in B.

triggered apoptosis primarily through mechanisms that engage the extrinsic pathway at an elevated level of caspase-8 (Fig. 7). Activation of caspase-8 results in activation of caspase-3, as shown by an increase in the cleavage of the specific caspase-3 substrate DEVD-AFC in PCV2-infected cells (Fig. 7). Caspase-3 cleaves ICAD (inhibitor of CAD [caspase-activated DNase]) and allows CAD to translocate to the nucleus and degrade DNA to ultimately produce the characteristic apoptotic phenotype of cell shrinkage, membrane blebbing, chromatin condensation, oligonucleosomal DNA fragmentation, and cell death (7, 13, 17, 32). Interestingly, transfection of cells with the ORF3 protein induced apoptosis using pathways (Fig. 9A and B) similar to those described in the context of viral infection. Furthermore, neither initiator caspase-8 and caspase-9 (data not shown) nor effector caspase-3 activities (Fig. 9C) were detected after infection with mutant PCV2 in the absence of ORF3 protein expression. Therefore, these results showed that PCV2 induced apoptosis in PK15 cells via a novel viral protein,

ORF3, through the activation of initiator caspase-8 followed by activation of the effector caspase-3 pathway.

Infection of pigs with PCV2 results in lymphocyte depletion of follicular and interfollicular areas together with macrophage infiltration of lymphoid tissues followed by immunosuppression (42). ORF2 has been considered a major capsid protein of PCV2 and could form virus-like particles after expression by a baculovirus-expressed system (31), indicating that other viral proteins of PCV2 might be nonstructural proteins which are not necessary for virion assembly. Moreover, the ORF2 protein has been shown to express at a high level in the late stage of infection when PCV2 was inoculated into VIDO R1 cells (23), as also demonstrated by us that the ORF2 protein expression peaked at 72 to 96 h postinfection in PCV2-infected PK15 cells (data not shown). In this study, ORF3 has been shown to have higher levels of expression at both the transcription and translation levels at 48 h in the PCV2-infected cells after infection (Fig. 1 and 2), suggesting that ORF3 might also
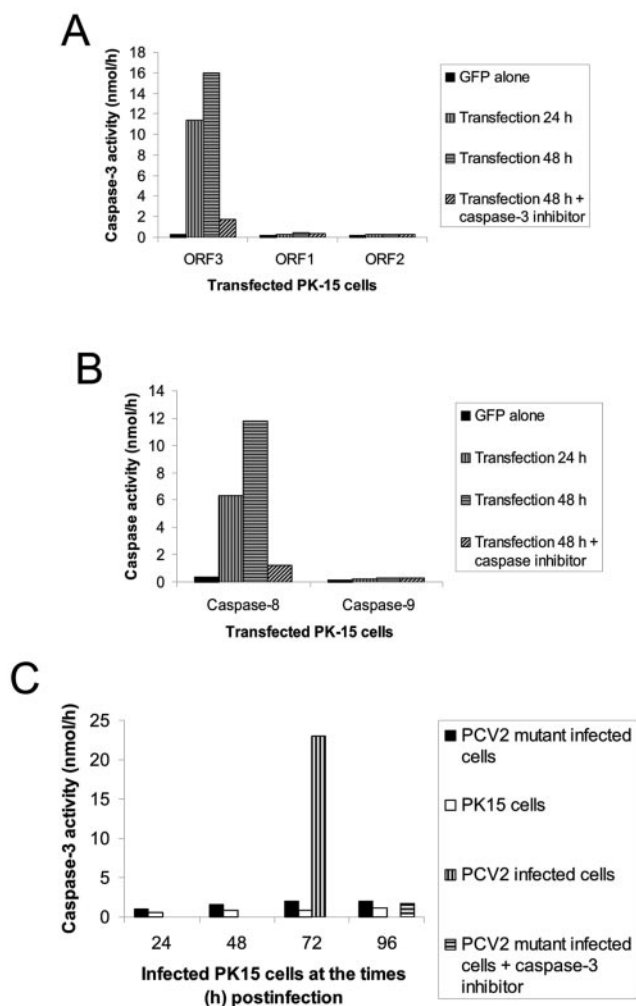
FIG. 9. ORF3 protein alone triggers apoptosis involving in caspase-8 activity. (A) Cell lysates were harvested at 24 and 48 h after transfection with GFP-ORF1, GFP-ORF2, or GFP-ORF3 plasmid and assayed for DEVDase activity using caspase-3 substrate DEVD-AFC. Mock-transfected cells as well as transfected cells treated with caspase-3 inhibitor DEVD-CHO were used as controls. The ORF3-transfected cells resulted in the cleavage of the caspase-3 substrate, whereas the ORF1- or ORF2-transfected cells cannot produce obvious caspase-3 activity similar to that in the mock-transfected cells. (B) Cell lysates were harvested at 24 and 48 h after transfection with GFP-ORF3 plasmid and assayed for IETDase or LEHDase activity using specific substrate IETD-AFC (caspase-8) or LEHD-AMC (caspase-9), respectively. Mock-transfected cells, as well as transfected cells treated with caspase-8 inhibitor IETD-fmk or caspase-9 inhibitor LEHD-CHO, were used as controls. The ORF3-transfceted cells resulted in the cleavage of caspase-8 but not of caspase-9 substrate. (C) Cell lysates were harvested at the different time points after infection with ORF3-deficient PCV2 and assayed for DEVDase activity using caspase-3 substrate DEVD-AFC. Mock-infected cells and PCV2-infected cells as well as ORF3-deficient PCV2-infected cells treated with caspase-3 inhibitor DEVD-CHO were used as controls. The caspase-3 activity in ORF3-deficient PCV2-infected cells remained stable and similar to that in mock-infected cells. All values shown are means from duplicated experiments.

be a nonstructural protein of PCV2. The nonstructural proteins of animal viruses might play an important role in viral replication and/or pathogenesis. For immunosuppressive virus, nonstructural protein VP3 of CAV was shown to cause apo-

ptosis in lymphoblastoid T cells and was implicated in pathogenesis (34); nonstuctural protein VP5 of chicken infectious bursal disease virus is not essential for viral replication (29) but was found to be involved in viral pathogenesis by its apoptotic activity (53). In our studies, we showed that the ORF3 protein of PCV2 is not required for viral replication in vitro and that PCV2-induced apoptotic activity was significantly reduced due to the absence of ORF3 protein expression. Our data also suggested that the expression of the ORF3 protein alone could induce apoptosis in transfected cells by activating the initiator caspase-8 pathway followed by activation of the effector caspase-3 pathway similar to that in PCV2-infected cells. Together, the ORF3 protein might play a role in viral pathogenesis by its apoptotic activity. Induction of apoptosis of immune system cells might be one of the requirements for virus-induced immunosuppression (12), and this might facilitate the use of the ORF3-deleted mutant as a potential live vaccine strain against PCV2 infection. However, whether the use of such ORF3 protein-deficient viruses can cause immunosuppression in pigs remains to be further determined.

In conclusion, ORF3 is a novel PCV2 protein that is not essential for viral replication in cultured PK15 cells and plays a major role in PCV2-induced apoptosis in cultured cells by activating initiator caspase-8 and effector caspase-3 pathways.

REFERENCES

1. **Allan, G. M., and J. A. Ellis.** 2000. Porcine circoviruses: a review. J. Vet. Diagn. Investig. **12:**3–14.
2. **Allan, G. M., S. Kennedy, F. McNeilly, J. C. Foster, J. A. Ellis, S. J. Krakowka, B. M. Meehan, and B. M. Adair.** 1999. Experimental reproduction of severe wasting disease by co-infection of pigs with porcine circovirus and porcine parvovirus. J. Comp. Pathol. **121:**1–11.
3. **Allan, G. M., F. McNeilly, J. P. Cassidy, G. A. Reilly, B. Adair, W. A. Ellis, and M. S. McNulty.** 1995. Pathogenesis of porcine circovirus: experimental infections of colostrum deprived piglets and examination of pig foetal material. Vet. Microbiol. **44:**49–64.
4. **Ashkenazi, A., and V. M. Dixit.** 1998. Death receptors: signalling and modulation. Science **281:**1305–1308.
5. **Blanchard, P., D. Mahé, R. Cariolet, A. Keranflec'h, M. A. Baudouard, P. Cordioli, E. Albina, and A. Jestin.** 2003. Protection of swine against post-weaning multisystemic wasting syndrome (PMWS) by porcine circovirus type 2 (PCV2) proteins. Vaccine **21:**4565–4575.
6. **Bolin, S. R., W. C. Stoffregen, G. P. Nayar, and A. L. Hamel.** 2001. Postweaning multisystemic wasting syndrome induced after experimental inoculation of cesarean-derived, colostrum-deprived piglets with type 2 porcine circovirus. J. Vet. Diagn. Investig. **13:**185–194.
7. **Budihardjo, I., H. Oliver, M. Lutter, and X. D. Wang.** 1999. Biochemical pathways of caspase activation during apoptosis. Annu. Rev. Cell Dev. Biol. **15:**269–290.
8. **Chae, C.** 2004. Postweaning multisystemic wasting syndrome: a review of aetiology, diagnosis and pathology. Vet. J. **168:**41–49.
9. **Cheung, A. K.** 2003. Transcriptional analysis of porcine circovirus type 2. Virology **305:**168–180.
10. **Cheung, A. K.** 2003. Comparative analysis of the transcriptional patterns of pathogenic and nonpathogenic porcine circoviruses. Virology **310:**41–49.
11. **Cohen, G. M.** 1997. Caspases: the executioners of apoptosis. Biochem. J. **326:**1–16.
12. **Drew, T. W.** 2000. A review of evidence for immunosuppression due to porcine reproductive and respiratory syndrome virus. Vet. Res. **31:**27–39.
13. **Earshaw, W. C., L. M. Martins, and S. H. Kaufmann.** 1999. Mammalian caspases: structure, activation, substrates, and functions during apoptosis. Annu. Rev. Biochem. **69:**383–424.
14. **Fenaux, M., P. G. Halbur, G. Haqshenas, R. Royer, P. Thomas, P. Nawagitgul, M. Gill, T. E. Toth, and X. J. Meng.** 2002. Cloned genomic DNA of type 2 porcine circovirus is infectious when injected directly into the liver and

lymph nodes of pigs: characterization of clinical disease, virus distribution, and pathologic lesions. J. Virol. **76:**541–551.

15. **Fenaux, M., T. Opriessnig, P. G. Halbur, and X. J. Meng.** 2003. Immunogenicity and pathogenicity of chimeric infectious DNA clones of pathogenic porcine circovirus type 2 (PCV2) and nonpathogenic PCV1 in weaning pigs. J. Virol. **77:**11232–11243.

16. **Green, D. R.** 1998. Apoptotic pathways: the roads to ruin. Cell **94:**695–698.

17. **Janicke, R. U., M. L. Sprengart, M. R. Wati, and A. G. Porter.** 1998. Caspase-3 is required for DNA fragmentation and morphological changes associated with apoptosis. J. Biol. Chem. **273:**9357–9360.

18. **Jeurissen, S. H., F. Wagenaar, J. M. Pol, A. J. Van der Eb, and M. H. M. Noteborn.** 1992. Chicken anemia virus causes apoptosis of thymocytes after in vivo infection and of cell lines after in vitro infection. J. Virol. **66:**7383–7388.

19. **Kamstrup, S., A. M. Barfoed, T. H. Frimann, A.-S. Ladekjær-Mikkelsen, and A. Bøtner.** 2004. Immunisation against PCV2 structural protein by DNA vaccine of mice. Vaccine **22:**1358–1361.

20. **Kennedy, S., D. Moffett, F. McNeilly, B. Meehan, J. Ellis, S. Krakowka, and G. M. Allan.** 2000. Reproduction of lesions of postweaning multisystemic wasting syndrome by infection of conventional pigs with porcine circovirus type 2 alone or in combination with porcine parvovirus. J. Comp. Pathol. **122:**9–24.

21. **Kiupel, M., G. W. Stevenson, J. Choi, K. S. Latimer, C. L. Kanitz, and S. K. Mittal.** 2001. Viral replication and lesions in BALB/c mice experimentally inoculated with porcine circovirus isolated from a pig with postweaning multisystemic wasting disease. Vet. Pathol. **38:**74–82.

22. **Lekcharoensuk, P., I. Morozov, P. S. Paul, N. Thangthumniyom, W. Wajjawalku, and X. J. Meng.** 2004. Epitope mapping of the major capsid protein of type 2 porcine circovirus (PCV2) by using chimeric PCV1 and PCV2. J. Virol. **78:**8135–8145.

23. **Liu, Q. G., S. K. Tikoo, and L. A. Babiuk.** 2001. Nuclear localization of the ORF2 protein encoded by porcine circovirus type 2. Virology **285:**91–99.

24. **Mandrioli, L., G. Sarli, S. Panarese, S. Baldoni, and P. S. Marcato.** 2004. Apoptosis and proliferative activity in lymph node reaction in postweaning multisystemic wasting syndrome (PMWS). Vet. Immunol. Immunopathol. **97:**25–37.

25. **Mankertz, A., R. Çaliskan, K. Hattermann, B. Hillenbrand, P. Kurzendoerfer, B. Mueller, C. Schmitt, T. Steinfeldt, and T. Finsterbusch.** 2004. Molecular biology of porcine circovirus: analyses of gene expression and viral replication. Vet. Microbiol. **98:**81–88.

26. **Mankertz, A., J. Mankertz, K. Wolf, and H. J. Buhk.** 1998. Identification of a protein essential for replication of porcine circovirus. J. Gen. Virol. **79:**381–383.

27. **Meehan, B. M., J. L. Creelan, M. S. McNulty, and D. Todd.** 1997. Sequence of porcine circovirus DNA: affinities with plant circoviruses. J. Gen. Virol. **78:**221–227.

28. **Miyata, H., H. Tsunoda, A. Kazi, A. Yamada, M. A. Khan, J. Murakami, T. Kamahora, K. Shiraki, and S. Hino.** 1999. Identification of a novel GC-rich 113-nucleotide region to complete the circular, single-stranded DNA genome of TT virus, the first human circovirus. J. Virol. **73:**3582–3586.

29. **Mundt, E., B. Köllner, and D. Kretzschmar.** 1997. Vp5 of infectious bursal disease virus is not essential for viral replication in cell culture. J. Virol. **71:**5647–5651.

30. **Nawagitgul, P., P. A. Harms, I. Morozov, B. J. Thacker, S. D. Sorden, C. Lekcharoensuk, and P. S. Paul.** 2002. Modified indirect porcine circovirus (PCV) type 2-based and recombinant capsid protein (ORF2)-based enzyme-linked immunosorbent assay for detection of antibodies to PCV. Clin. Diagn. Lab. Immunol. **9:**33–40.

31. **Nawagitgul, P., I. Morozov, S. R. Bolin, P. A. Harms, and S. D. Sorden.** 2000. Open reading frame 2 of porcine circovirus type 2 encodes a major capsid protein. J. Gen. Virol. **81:**2281–2287.

32. **Nicholson, D. W., A. Ali, N. A. Thornberry, J. P. Vaillancourt, C. K. Ding, M. Gallant, Y. Gareau, P. R. Griffin, M. Labelle, Y. A. Lazebnik, N. A. Munday, S. M. Raju, M. E. Smulson, T.-T. Yamin, V. L. Yu, and D. K. Miller.** 1995.

33. **Nishizawa, T., H. Okamoto, K. Konishi, H. Yoshizawa, Y. Miyakawa, and M. Mayumi.** 1997. A novel DNA virus (TTV) associated with elevated transaminase levels in posttransfusion hepatitis of unknown etiology. Biochem. Biophys. Res. Commun. **241:**92–97.

34. **Noteborn, M. H. M., D. Todd, C. A. Verschueren, H. W. de Gauw, W. L. Curran, S. Veldkamp, A. J. Douglas, M. S. McNulty, A. J. Van der Eb, and G. Koch.** 1994. A single chicken anemia virus protein induces apoptosis. J. Virol. **68:**346–351.

35. **Phenix, K. V., J. H. Weston, I. Ypelaar, A. Lavazza, J. A. Smyth, D. Todd, G. E. Wilcox, and S. R. Raidal.** 2001. Nucleotide sequence analysis of a novel circovirus of canaries and its relationship to other members of the genus Circovirus of the family Circoviridae. J. Gen. Virol. **82:**2805–2809.

36. **Pringle, C. R.** 1999. Virus taxonomy at the XIth International Congress of Virology, Sydney, Australia. Arch. Virol. **144:**2065–2070.

37. **Resendes, A. R., N. Majó, J. Segalés, E. Mateu, M. Calsamiglia, and M. Domingo.** 2004. Apoptosis in lymphoid organs of pigs naturally infected by porcine circovirus type 2. J. Gen. Virol. **85:**2837–2844.

38. **Ritchie, B. W., F. D. Niagro, P. D. Lukert, W. L. Steffens III, and K. S. Latimer.** 1989. Characterization of a new virus from cockatoos with psittacine beak and feather disease. Virology **171:**83–88.

39. **Roulston, A., R. C. Marcellus, and P. E. Branton.** 1999. Virus and apoptosis. Annu. Rev. Microbiol. **53:**577–628.

40. **Salvesen, G. S., and V. M. Dixit.** 1997. Caspases: intracellular signaling by proteolysis. Cell **91:**443–446.

41. **Schulze-Osthoff, K., D. Ferrari, M. Los, S. Wesselborg, and M. E. Peter.** 1998. Apoptosis signalling by death receptors. Eur. J. Biochem. **254:**439–459.

42. **Segalés, J., M. Domingo, F. Chianini, N. Majó, J. Domínguez, L. Darwich, and E. Mateu.** 2004. Immunosuppression in postweaning multisystemic wasting syndrome affected pigs. Vet. Microbiol. **98:**151–158.

43. **Shibahara, T., K. Sato, Y. Ishikawa, and K. Kadota.** 2000. Porcine circovirus induces B lymphocyte depletion in pigs with wasting disease syndrome. J. Vet. Med. Sci. **62:**1125–1131.

44. **Takahashi, K., Y. Iwasa, M. Hijikata, and S. Mishiro.** 2000. Identification of a new human DNA virus (TTV-like mini virus, TLMV) intermediately related to TT virus and chicken anemia virus. Arch. Virol. **145:**979–993.

45. **Telford, W. G., L. E. King, and P. J. Fraker.** 1992. Comparative evaluation of several DNA binding dyes in the detection of apoptosis-associated chromatin degradation by flow cytometry. Cytometry **13:**137–143.

46. **Teodoro, J. G., and P. E. Branton.** 1997. Regulation of apoptosis by viral gene products. J. Virol. **71:**1739–1746.

47. **Tischer, I., H. Gelderblom, W. Vettermann, and M. A. Koch.** 1982. A very small porcine virus with circular single-stranded DNA. Nature **295:**64–66.

48. **Tischer, I., W. Mields, D. Wolff, M. Vagt, and W. Griem.** 1986. Studies on epidemiology and pathogenicity of porcine circovirus. Arch. Virol. **91:**271–276.

49. **Tischer, I., D. Peters, R. Rasch, and S. Pociuli.** 1987. Replication of porcine circovirus: induction by glucosamine and cell cycle dependence. Arch. Virol. **96:**39–57.

50. **Todd, D., F. D. Niagro, B. W. Ritchie, W. Curran, G. M. Allan., P. D. Lukert., K. S. Latimer, W. L. Steffens III, and M. S. McNulty.** 1991. Comparison of three animal viruses with circular single-stranded DNA genomes. Arch. Virol. **117:**129–135.

51. **Todd, D., J. H. Weston, D. Soike, and J. A. Smyth.** 2001. Genome sequence determinations and analyses of novel circoviruses from goose and pigeon. Virology **286:**354–362.

52. **Woods, L. W., K. S. Latimer, B. C. Barr, F. D. Niagro, R. P. Campagnoli, R. W. Nordhausen, and A. E. Castro.** 1993. Circovirus-like infection in a pigeon. J. Vet. Diagn. Investig. **5:**609–612.

53. **Yao, K., and V. N. Vakharia.** 2001. Induction of apoptosis in vitro by the 17-kDa nonstructural protein of infectious bursal disease virus: possible role in viral pathogenesis. Virology **285:**50–58.

Identification and inhibition of the ICE/CED-3 protease necessary for mammalian apoptosis. Nature **376:**37–43.